Progress In Electromagnetics Research C, Vol. 138, 117–129, 2023

A Printed Monopole Antenna for Next Generation Internet of Things: Narrow-Band Internet of Things (NB-IoT)

Sneha Bhardwaj[1], Praveen K. Malik[1], Tanvir Islam[2], Anita Gehlot[3], Sudipta Das[4, *], and Sivaji Asha[5]

Abstract—This article introduces a planar monopole antenna specially designed for NB-IoT module devices. The preferred choice for Internet of Things (IoT) technology is the Narrow-Band Internet of Things (NB-IoT) due to its extensive coverage and low power consumption. NB-IoT is specifically designed for IoT applications. A circular patch antenna with dimensions of 30 mm × 60 mm is fabricated, which is specifically tailored for the NB-IoT module. The antenna dimensions are meticulously chosen to ensure compatibility with the device module, considering the NB-IoT B1 (2100) and B3 (1800) frequency bands. Among various patch shapes, the circular design is preferred for its advantages over hexagon and square patches. The desired antenna configuration combines a square-slotted patch with a monopole ground plane, and it offers several advantages in terms of design simplicity, compact size, and characteristics such as broad bandwidth, acceptable gain, and high radiation efficiency. The design process employs HFSS Software and utilizes an FR4 substrate of 1.6 mm thickness. Operating at resonance frequencies of 2.1 GHz and 1.8 GHz, the antenna covers a broad frequency spectrum of 1100 MHz (1.5 to 2.6 GHz) with a fractional bandwidth of 53.65%. The suggested antenna achieves a peak gain of 3.3 dB and maximum radiation efficiency of 96% within its operating band. It exhibits an omnidirectional radiation pattern, meeting the specific requirements of NB-IoT technologies. Experimental measurements of the fabricated antenna validate the results achieved from the simulated data.

1. INTRODUCTION

Narrowband IoT technology provides a broad range of connectivity to IoT devices, which can easily communicate a few bits of data over a wide range. It is a wireless communication standard specifically designed for connecting IoT devices. It operates in the licensed spectrum, which ensures interference-free communication and improved security. NB-IoT utilizes existing cellular infrastructure to provide reliable and cost-effective connectivity for a wide range of IoT applications. The NB-IoT communication needs very little power for data communication, which leads to an increase in the battery life to more than 10 years. Various useful features of NB-IoT make it well suited for many applications like automation of systems or smart systems as displayed in Figure 1 [1]. The NB-IoT communication spectrum utilizes B3 and B1 bands and is in high demand for tracking, sensing, and monitoring [2, 3]. To function effectively, NB-IoT requires sensor nodes, a robust communication network, and compatible application devices that can access data via cloud servers and other devices [4]. NB-IoT antennas play a critical role, necessitating

Received 2 September 2023, Accepted 30 September 2023, Scheduled 7 October 2023
* Corresponding author: Sudipta Das (sudipta.das1985@gmail.com).
[1] Department of Electronics and Communication, Lovely Professional University, Jalandhar, India. [2] Department of Electrical and Computer Engineering, University of Houston, Houston, TX 77204, USA. [3] Division of Research and Innovation, Uttaranchal University, Dehradun, Uttrakhand 248007, India. [4] Department of Electronics and Communication Engineering, IMPS College of Engineering and Technology, Malda-732103, West Bengal, India. [5] Saveetha Engineering College, Saveetha Nagar, Thandalam, Chennai-602105, India.

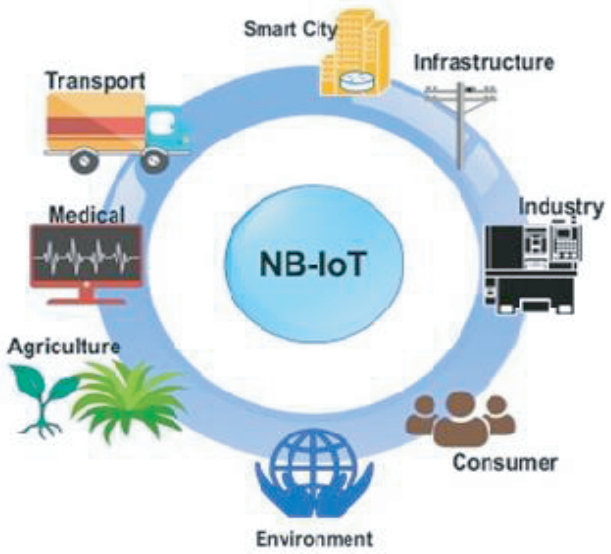

Figure 1. NB-IoT Applications where NB-IoT helps to make smart cities and environments.

specific attributes: operating within narrowband frequencies (800–900 MHz or 1.8–2.2 GHz), substantial amplification for long-distance communication, narrow beam width for directional coverage, compact size, low power consumption, and optimal impedance matching. Recent advancements involve planar microstrip patch antennas to address NB-IoT and IoT frequency requirements [5–11]. There are several types of NB-IoT (Narrowband Internet of Things) antennas designed to cater to various deployment scenarios and communication needs. One common type is the Printed Circuit Board (PCB) antenna, which is compact and cost-effective, making it suitable for small IoT devices with limited space [12, 13]. On the other hand, external antennas, such as dipole and monopole antennas, provide better signal reception and transmission capabilities and are often used in outdoor or industrial applications where range and reliability are critical [14]. Additionally, magnetic mount antennas are versatile options for IoT devices that need to be easily attached to metal surfaces [15]. Each of these NB-IoT antenna types offers unique advantages, allowing IoT designers to select the most appropriate solution for their specific use cases. Mostly, dual-band antenna has the disadvantages of complex structure, large patch, and low efficiency. Unlike a multiband antenna, which resonates at multiple bands with low bandwidth, broadband antenna resonates around the center frequency and covers multiple frequencies with broad bandwidth. To achieve broad bandwidth, a slot structure in patch and ground is used, which excites the antenna's multiple resonance modes [16–20].

The proposed compact antenna covers NB-IoT B1 and B3 bands and contributes to achieving broadband functionality. Consequently, the NB-IoT module system must design an antenna compatible with B1 and B5 bands. Existing research explores diverse antenna structures for IoT and wireless communication. One approach involves creating a triple-notched band UWB antenna by adding three band-stop filters to a circular-patch co-planar waveguide (CPW)-fed antenna on a silicon substrate [21]. The challenge of unconnected ground in Multiple-Input Multiple-Output (MIMO) technology is addressed in [22] by connecting all grounds to establish common potential. Common patches are also utilized in MIMO technology [23]. Multiband microstrip antennas are designed for Global Systems for Mobile (GSM) Communications and Long-Term Evolution (LTE) applications by incorporating complementary split-ring resonators [24] and meander lines for 5.80 GHz WLAN applications [25]. Another compact multiband antenna, fabricated on an FR4 substrate, extracts three resonances for Worldwide Interoperability for Microwave Access (WiMAX) applications [26]. Additionally, researchers propose rectenna antennas for energy harvesting [27] and employ metamaterials to minimize antenna dimensions [28, 29]. Slot-based microstrip antennas find extensive use in wireless communication, including IoT applications [30–37]. In this article, a small size, slotted circular patch is designed for IoT applications. The proposed antenna can be operated for NB-IoT applications in the B1 and

B3 bands. The prototype is designed and fabricated on an FR4 substrate with a relative permittivity 4.4, loss tangent 0.025, and thickness 1.6 mm. The designed antenna prototype is manufactured, and measurements are performed to validate the simulation results.

The primary achievement of this research can be described as:

i. Integration Friendly Compact Size: The antenna introduced in this study possesses a compact size, distinguishing it from previously documented antennas in the academic literature. This compactness is advantageous for applications where space is limited, such as in small electronic devices and sensors. Due to its small physical size, this antenna can be seamlessly integrated into an NB-IoT modules without consuming excessive space or impeding the overall functionality of the device. This feature is critical for designing compact and efficient IoT devices.

ii. Frequency Band Compatibility: This antenna's operational range effectively covers the B1 and B3 bands of NB-IoT, indicating its suitability for integration into multi-antenna systems that require coverage within these specific frequency bands. This compatibility enhances its versatility in IoT applications.

iii. Simple Design for Ease of Fabrication: The antenna's design is characterized by its simplicity, making it relatively easy and cost-effective to manufacture. This design simplicity is vital for mass production, reducing production costs, and ensuring consistency in antenna performance across a production batch.

iv. Enhanced Bandwidth via Slot and Reduced Footprint: To achieve an enhanced bandwidth, the antenna design incorporates a slot, which expands the range of frequencies that it can transmit and receive. Additionally, the removal of peripheral edges from the circular patch reduces the antenna's physical footprint while preserving its performance. This dual optimization strategy results in a smaller antenna that maintains its effectiveness, ideal for space-constrained IoT applications.

Section 2 of the study focuses on the patch design and the impact of the slot on the patch antenna. Detailed parametric studies are presented in Section 3, aiming to optimize the size and performance of the antenna. Section 4 elaborates the fabrication process and antenna measurement. Finally, the concluding section summarizes the findings and contributions of the article.

2. DESIGN METHODS AND SPECIFICATIONS

The design is presented in Figure 2, and the specified dimensions are $L_s = 60\,\text{mm}$, $W_s = 30\,\text{mm}$, $L_{slot} = 12\,\text{mm}$, $W_{slot} = 12\,\text{mm}$, $R = 17.5\,\text{mm}$, $L_f = 30\,\text{mm}$, $W_f = 5\,\text{mm}$, $L_c = 16\,\text{mm}$, $L_{dgs} = 6\,\text{mm}$, $W_{dgs} = 9\,\text{mm}$, and $L_g = 30\,\text{mm}$. The length of the ground has been adjusted to achieve impedance matching with the monopole, and it is connected through a microstrip feed line. To enhance impedance matching and optimize the antenna's radiation efficiency, a slot has been introduced in the ground plane. The designed structure was simulated using the Ansoft High-Frequency Structure Simulator (HFSS). Furthermore, a square slot has been integrated into the patch, resulting in a second resonance frequency within the B3 frequency band. The initial design involves a circular patch monopole antenna that is fed using a microstrip line. It resonates at approximately 2.1 GHz but has a narrow bandwidth limited to the B1 band of NB-IoT. The resonance at 2.1 GHz is not optimal for the geometry depicted in Figure 3(a), due to a mismatch between the feed line and the patch. To overcome the discrepancy in impedance, a slot is implemented within the ground structure as illustrated in Figure 3(b). A square slot is integrated into the upper patch, leading to an extra resonance at 1.8 GHz, as depicted in Figure 3(c). The concluding procedure involves trimming the outer circular patch to decrease its dimensions by 4 mm $\times$ 2 mm while ensuring no adverse effects on the antenna's performance mentioned in Figure 3(d).

In Figure 4(a), the reflection coefficient values for all the designs are provided, and gain versus frequency is also mentioned in Figure 4(b). Before considering the circular patch for the proposed design, the square and hexagon patches are also studied. The circular patch design offers several advantages compared to square and hexagon patches when the substrate and ground plane dimensions are considered. The width of the feed line is adjusted accordingly to achieve the desired impedance. From Figure 5, we can say that the hexagonal patch shows a larger impedance bandwidth, but the maximum gain is achieved with the circular patch, as shown in Figure 6.

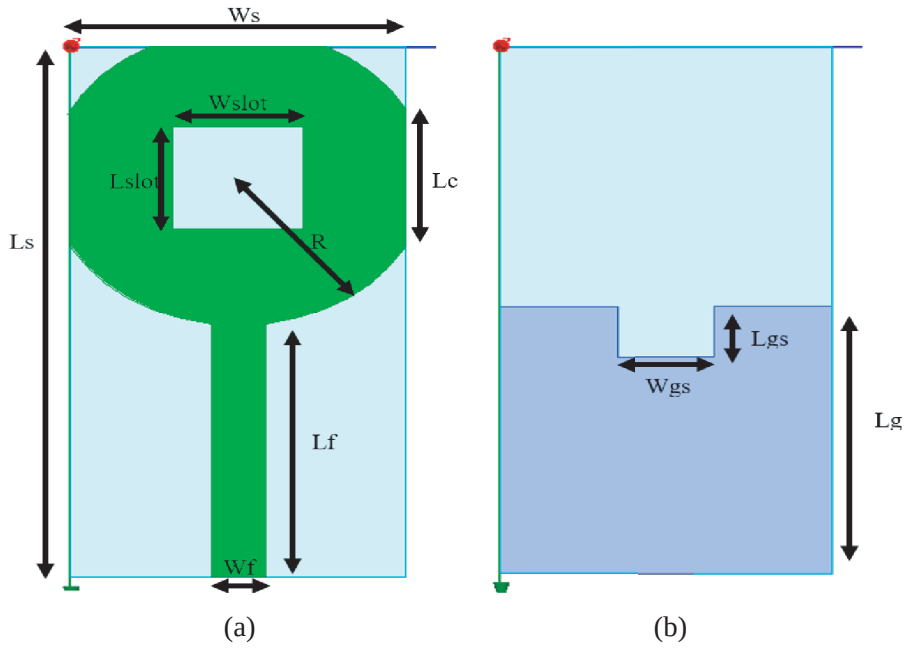

Figure 2. Antenna geometry. (a) Top, (b) bottom view.

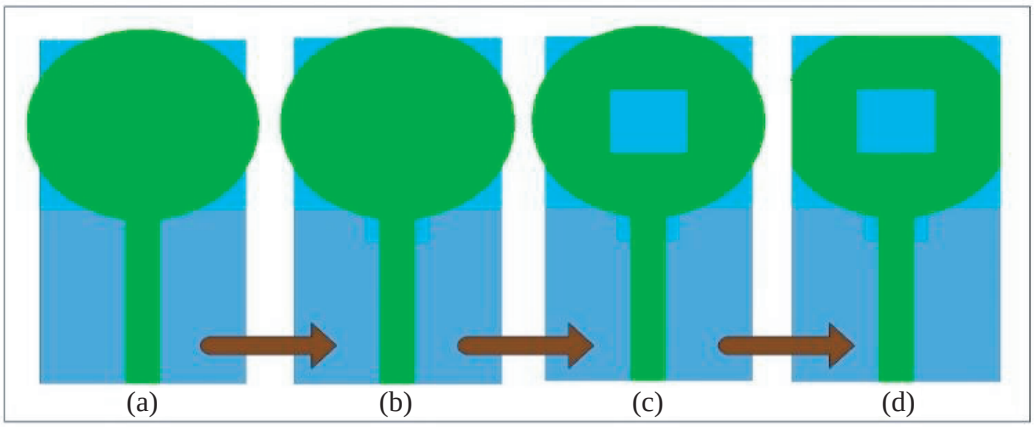

Figure 3. Modification in design structure step-wise (green-upper patch and grey-ground plane).

Consequently, for our specific requirements regarding bandwidth and gain, the circular patch design is deemed the most suitable. The circular patch design offers advantages over square and hexagon patches with the same substrate and ground plane dimensions, ensuring impedance matching by adjusting the feed line width. The hexagonal patch exhibits a larger impedance bandwidth, while the circular patch achieves the maximum gain. Consequently, for our requirements, the circular patch design is chosen due to its optimal performance in terms of bandwidth and gain.

3. PARAMETRIC STUDIES

To enhance the performance of the design and achieve an optimal antenna size, a thorough investigation has been conducted. The following parameters are also identified as having an effective impact on the antenna's performance.

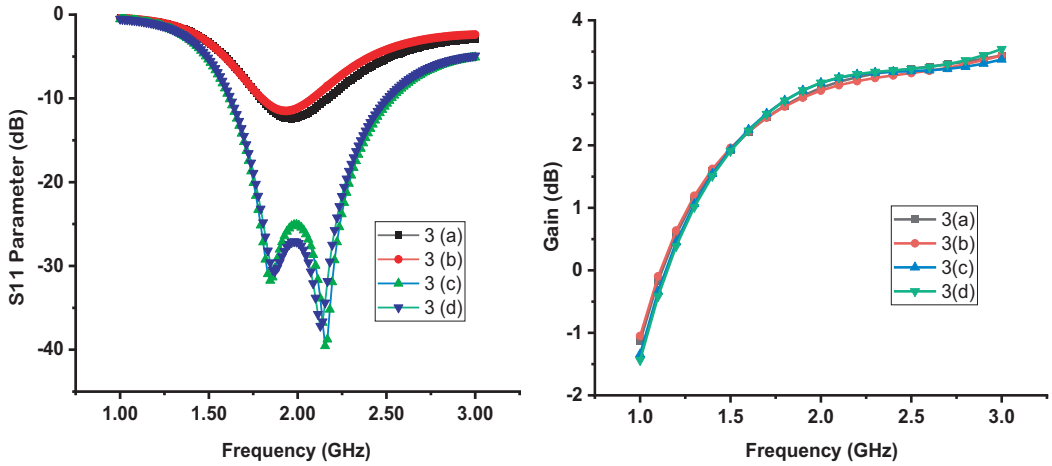

(a) (b)

Figure 4. (a) S_{11} graph, (b) gain plot for the modified patch design.

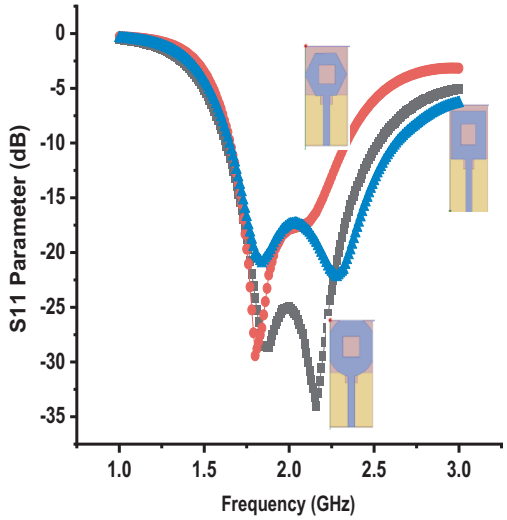

Figure 5. S_{11} comparison for different patch shapes.

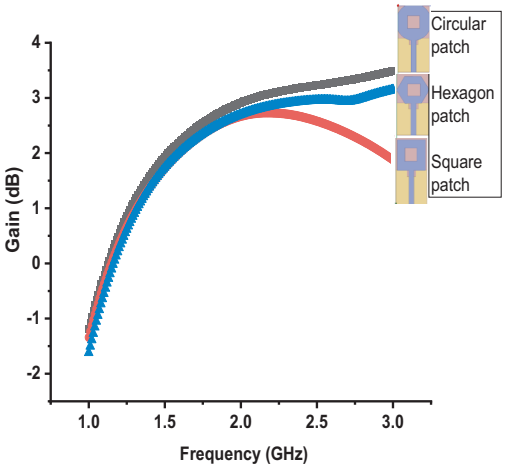

Figure 6. Gain (dB) comparison for different patch shapes.

3.1. Feed Line Width (W_f)

The input impedance of an antenna is a crucial factor that is affected by the width of the feed line, as illustrated in Figure 7. These two parameters are inversely correlated, meaning that a change in the width of the feed line will have an impact on the return loss of the antenna. In the design process, the patch dimension and dielectric substrate are chosen, and initially, the microstrip line width is calculated using Equation (1) [38]. A width of 12 mm is selected as a trade-off between achieving a perfect match and ensuring sufficient bandwidth. Alternatively, an online width calculator can be utilized to determine the appropriate width dimension [39].

Formula to find the width of the feed line [21]

$$Z_c = \frac{60}{\sqrt{\varepsilon_{reff}}} \ln\left[\frac{8h}{W_o} + \frac{W_o}{4h}\right] \quad if \ \frac{W_o}{h} \leq 1 \tag{1}$$

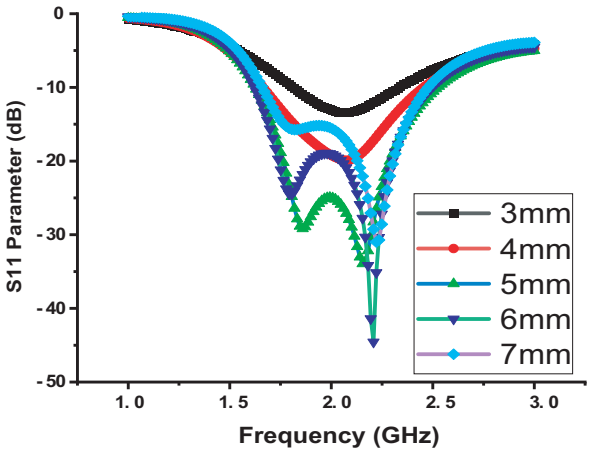

Figure 7. The S_{11} plot for different values of width.

and

$$Z_c = \frac{120\pi}{\sqrt{\varepsilon_{reff}}\left[\frac{W_o}{h}+1.393+0.667\ln\left(\frac{W_o}{h}+1.444\right)\right]} \quad if\ \frac{W_o}{h} > 1 \tag{2}$$

where "Z_c = characteristics impedance of feed line as we have a 50 ohm connector feed, so mostly it will be 50 ohms for a perfect match. h = height of substrate. ε_{reff} = effective dielectric constant".

3.2. Width of Square Slot (L_{slot}, W_{slot})

The geometric configuration of the antenna aperture plays a crucial role in achieving impedance matching and electromagnetic coupling with the patch element. Upon examination of the reflection coefficient plot represented in Figure 8, it can be deduced that the dimensions of the slot do not affect the resonant frequency, but they do have an impact on the antenna's impedance characteristics. Generally, wider slots exhibit a wider operating bandwidth; nevertheless, their smaller dimensions impose limitations on the extent of bandwidth enhancement [39]. Modifying the slot dimensions during the patch design process affects the distribution of electric current, thereby causing alterations in the impedance and ultimately influencing the resonant behavior. In this study, the size of the square slot was changed between 10 mm and 14 mm, and the best size was found to be 12 mm.

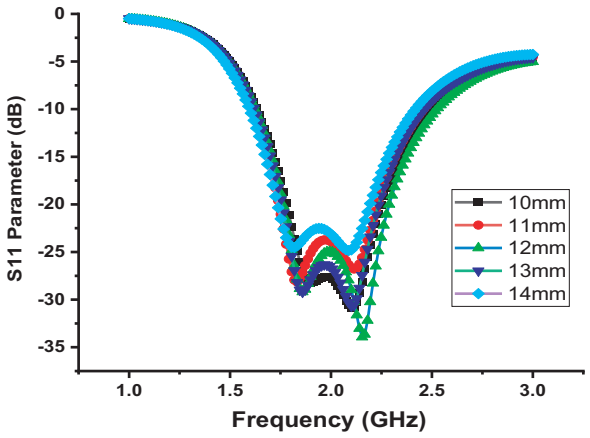

Figure 8. The S_{11} plot for different values of the square slot.

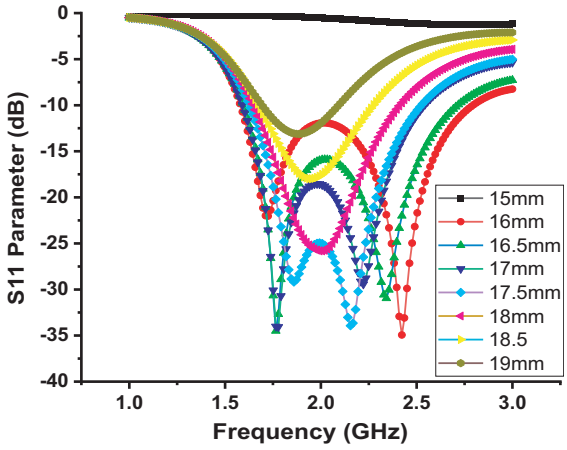

Figure 9. S_{11} plot for different values of radius of circular patch.

3.3. Circular Patch Radius (R)

When the size of the circular patch is altered, it affects the resonant length of the antenna, consequently modifying its resonant frequency. Figure 9 provides a visual representation of the changes in resonant frequency. To ensure compatibility with the NB-IoT Module chip and meet the desired frequency specifications, a radius of 17.5 mm is chosen after optimization. The study involves exploring the parametric range of 15 mm to 19 mm in 0.5 mm increments.

3.4. Ground Structure Slot (L_{gs} & W_{gs})

To enhance the impedance matching between the antenna and the feed line, a slot is added within the ground structure where the feed line and antenna are connected. This slot improves the coupling between the two structures, resulting in improved impedance matching. However, it is worth noting that excessive coupling can negatively impact the antenna's performance [40]. In the parametric study, the length and width of the hole in the ground structure are changed at the same time. This is done to optimize the antenna for perfect impedance matching. The optimized slot size is determined to be 6 mm × 9 mm, as depicted in Figure 10.

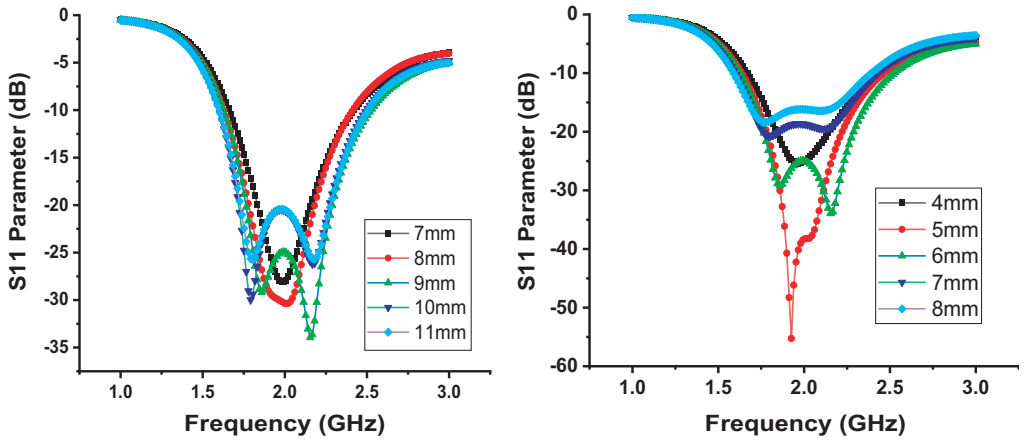

Figure 10. S_{11} graph for different values of slot designed in-ground, (a) length, (b) width.

The input impedance of an antenna is influenced by various design parameters, such as the width of the feed line, slot size, and radius of the circular patch. By carefully selecting and optimizing these parameters, achieving the desired impedance matching and resonance frequency for the antenna is possible. The design process involves evaluating the trade-offs among perfect match, bandwidth, size availability, and frequency requirements. Through parametric studies and simulations, the optimal dimensions for the microstrip line, slot, and patch can be determined, ensuring the antenna's efficient performance in terms of impedance, resonance, and bandwidth.

4. RESULTS AND DISCUSSIONS

This section provides a comprehensive overview of the fabricated antenna and its performance, emphasizing technical details. Figure 11 depicts the physical structure of the antenna. To evaluate the antenna's characteristics, the S_{11} parameters were measured using the E8362C PNA Microwave Network Analyzer, as illustrated in Figure 12. S_{11} refers to the reflection coefficient, which measures the degree of matching between the antenna's port and feed line. It serves as an indicator of how effectively the antenna transmits electromagnetic waves.

Figure 13 presents a comparison between simulated and measured data of S_{11} parameters. The bandwidth, spanning from 1.5 GHz to 2.6 GHz, encompasses the NB-IoT's B1 and B3 frequency bands. Utilizing a microwave network analyzer, we measured S_{11} parameter (reflection coefficient), which agrees

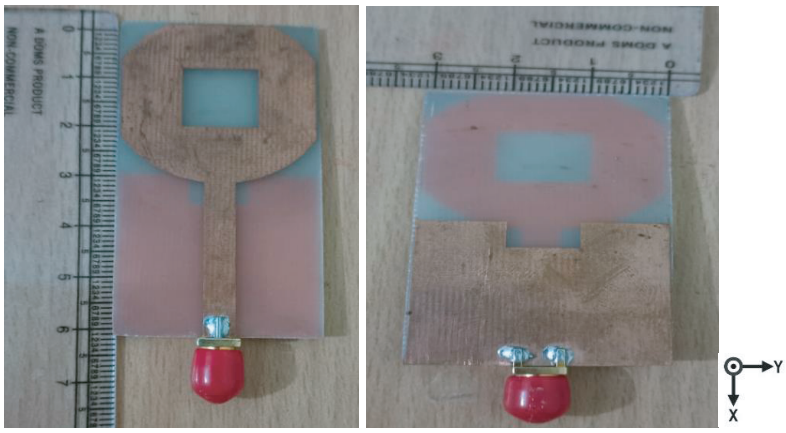

(a) (b)

Figure 11. Fabricated antenna structure top, (a) and bottom, (b) view.

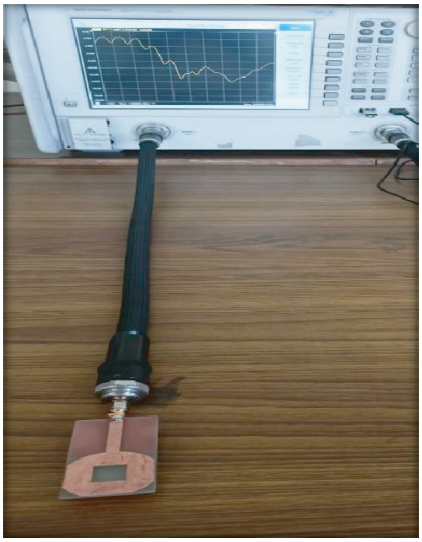

Figure 12. A fabricated antenna connected to VNA.

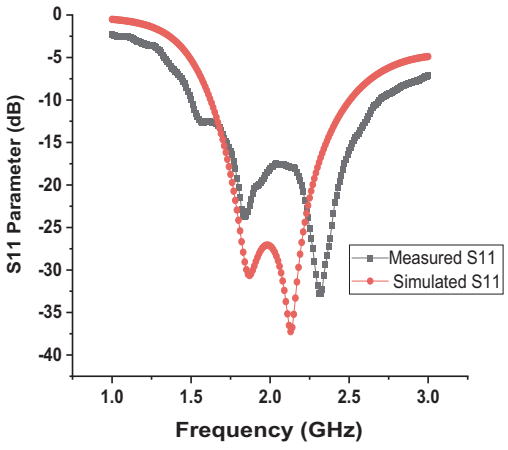

Figure 13. The S_{11} vs. frequency comparison.

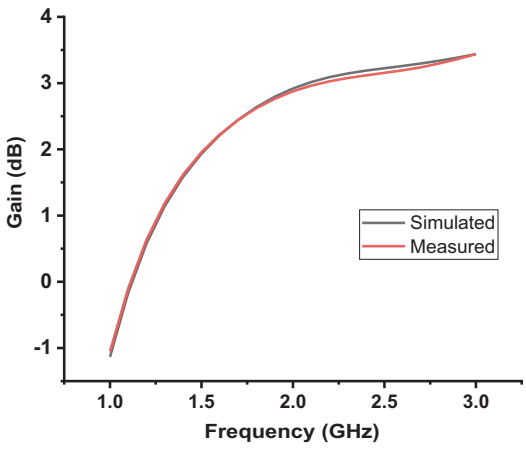

Figure 14. The simulated gain vs. frequency graph.

closely with the simulated results and hence confirms the antenna's bandwidth coverage for NB-IoT bands. The minor resonance deviations may be due to connector mismatches, potential manufacturing errors, or soldering issues.

Gain of the antenna, a parameter used to quantify an antenna's directional properties, indicates how well the antenna focuses its power in a specific direction. High-gain antennas exhibit strong directionality, while low-gain antennas radiate power evenly in all directions. In an ideal scenario, antennas would distribute power equally in all directions, resembling isotropic antennas. It is important to note that antennas do not generate power themselves; rather, they redistribute the existing power in various directions. Figure 14 presents the gain characteristics, comparing simulated and measured data to elucidate the relationship between gain and frequency. The graph demonstrates that the gain consistently exceeds 2 dB throughout the entire impedance bandwidth, peaking at 3.3 dB. In Figure 15(a), we observe the simulated radiation efficiency of the proposed antenna design, while Figure 15(b) depicts the surface current distribution at a 2 GHz frequency. Surface current, denoting the flow of electrical current on the antenna's conductor surface, governs the emission of electromagnetic waves. Analyzing this distribution is pivotal for designing optimal patch antennas to ensure efficient

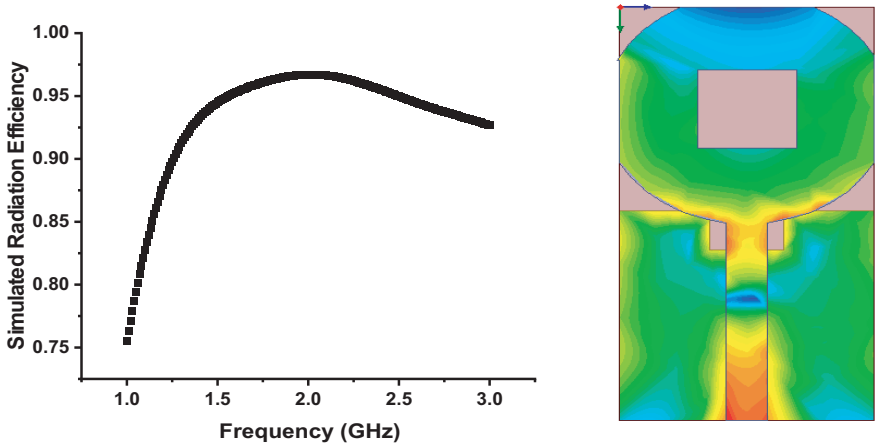

Figure 15. (a) Simulated radiation efficiency graph, (b) surface current density at 2 GHz.

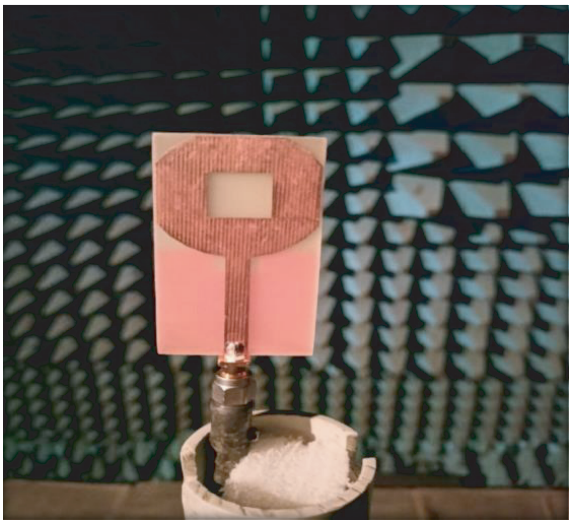

Figure 16. Photograph of the fabricated antenna in an anechoic chamber.

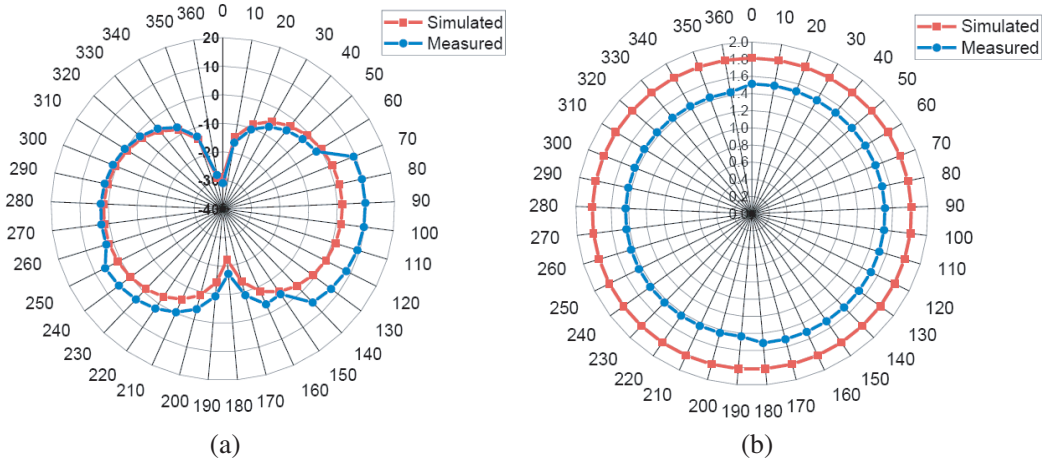

Figure 17. The simulated and measured radiation pattern, (a) *E*-Plane, (b) *H*-Plane at 2.1 GHz.

Table 1. Comparison of the proposed antenna with other published antennae.

Ref.	Design complexity or structure	Dimension (mm^3)	Substrate	Frequency bands (GHz)	Bandwidth (MHz)	Peak gain (dB)	Maximum Radiation efficiency
[11]	2-layer structure fed with twin -line balanced	0.48λ × 0.11λ × 0.01λ	Rogers RT 5880	1.8	40	–0.4	60%
[27]	Slotted Patch MIMO	0.32λ × 0.32λ × 0.01λ	FR4	1.73 & 2.53	30	–3.8	45%
[28]	Monopole patch metamaterial	0.32λ × 0.32λ × 0.017λ	FR4	1.1 & 1.6	180	–3.2 and 1.1	50% and 85%
[29]	Folded Dipole	0.32λ × 0.23λ × 0.01λ	FR4	2.1	100	2	90%
[30]	Switchable slot antenna	0.64λ × 0.64λ × 0.012λ	FR4	2.4	142	2.33	-
[31]	C-shaped conforming	1.67λ × 2.08λ × 0.012λ	FR4	1.8 & 2.4	100	4.4	85%
[32]	L-shaped CPW feed	0.44λ × 0.44λ × 0.12λ	FR4	2.4	3000	–0.5	-
[33]	Tuneable rectangular slot antenna	0.48λ × 0.24λ × 0.0125λ	Duroid 5880 (TM)	1.5	400	1	-
[34]	Meandered slot design loaded with varactor diode	0.1λ × 0.22λ × 0.002λ	RO4350	0.75 & 1.1	17	–0.35	70% at 1.1 GHz
[35]	Slotted square patch	0.29λ × 0.29λ × 0.12λ	FR4	2.4	220	3.2	-
Proposed Design	**Circular slotted patch**	**0.2λ × 0.4λ × 0.010λ**	**FR4**	**1.8 & 2.1**	**1100**	**3.3**	**96%**

signal transmission and reception. The antenna maintains above 92% radiation efficiency across the entire impedance bandwidth, and the maximum radiation efficiency is around 96%.

To measure the performance of the antenna, it was placed inside an anechoic chamber, as illustrated in Figure 16. The gain measurements were carried out employing the reference gain measurement method. To find out how directed the antenna is, Figure 17 shows E and H plane radiation patterns, calculated at 2.1 GHz. The simulated radiation pattern is represented by the red color plot, while the measured radiation pattern is depicted by the blue color plot. Based on the analysis, it can be observed that the proposed antenna demonstrates vertical linear polarization and an almost bidirectional radiation pattern in E plane and nearly omnidirectional radiation pattern in H plane. Additionally, the antenna possesses a wide beam width at half power at the central frequency, indicating its ability to radiate energy in omnidirections.

To showcase the benefits of the designed antenna, a comparative analysis is conducted between the proposed design and an existing design that operates within the same frequency range or is intended for NB-IoT applications. The specific details are presented in Table 1.

5. CONCLUSIONS

The fabricated antenna performs as intended, effectively covering both frequency bands. It maintains an impressive -10 dB impedance bandwidth from 1.5 GHz to 2.6 GHz with a 53.65% fractional bandwidth and radiation efficiency exceeding 92% within this range. Extensive analysis validates its suitability for NB-IoT applications, allowing seamless integration with existing mobile networks through software and system upgrades. This facilitates reliable data communication in wireless sensor networks and enables implementation in various modern communications. The utilization of NB-IoT also capitalizes on the inherent security and privacy features that the existing mobile network architecture offers. The proposed design can be incorporated with NB-IoT modules for future applications to support data communication. Additionally, optimizing the antenna's reception at the receiver side can be achieved by designing antennas with polarization purity, potentially implementing circular polarization through a power divider circuit. Moreover, the antenna's bandwidth can be expanded to encompass B5 bands by introducing a meta-surface ground structure to the antenna.

REFERENCES

1. HUAWEI, "NB-IoT enables new business opportunities," July 17, 2017, Available: http://www.huawei.com/minisite/IoT/img/nb_IoT_whitepaper_en.pdf.
2. Sneha, P. K. Malik, N. Bilandi, and A. Gupta, "Narrow band-IoT and long-range technology of IoT smart communication: Designs and challenges," *Computers & Industrial Engineering*, Vol. 172, 108572, 2022, https://doi.org/10.1016/j.cie.2022.108572.
3. Rastogi, E., N. Saxena, A. Roy, and D. R. Shin, "Narrowband internet of things: A comprehensive study," *Computer Networks*, Vol. 173, 107209, 2020, doi: 10.1016/j.comnet.2020.107209.
4. Mekki, K., E. Bajic, F. Chaxel, and F. Meyer, "A comparative study of LPWAN technologies for large-scale IoT deployment," *ICT Express*, Vol. 5, 1–7, 2019, doi: 10.1016/j.icte.2017.12.005.
5. Malik, P. K., D. S. Wadhwa, and J. S. Khinda, "A survey of device to device and cooperative communication for the future cellular networks," *International Journal of Wireless Information Networks*, Vol. 27, 411–432, 2020, doi:10.1007/s10776-020-00482-8.
6. Gupta, N. P., P. K. Malik, and B. S. Ram, "A review on methods and systems for early breast cancer detection," *International Conference on Computation, Automation and Knowledge Management (ICCAKM)*, 42–46, 2020.
7. Riaz, S., M. Khan, U. Javed, et al., "A miniaturized frequency reconfigurable patch antenna for IoT applications," *Wireless Pers. Commun.*, Vol. 123, 1871–1881, 2022, https://doi.org/10.1007/s11277-021-09218-0.
8. Jeyakumar, P., P. Muthuchidambaranathan, and S. Shrinidhi, "A novel two port high isolation dual-polarized multiband sub-6 GHz MIMO antenna for IoT connected devices," *Wireless Pers. Commun.*, Vol. 121, 2569–2587, 2021.

9. Bukhari, B. and G. M. Rather, "Multiband compact MIMO antenna for cognitive radio, IoT and 5G New radio sub 6 GHz applications," *Progress In Electromagnetics Research C*, Vol. 121, 265–279, 2022.
10. Raad, H. K., "An UWB antenna array for flexible IoT wireless systems," *Progress In Electromagnetics Research*, Vol. 162, 109–121, 2018.
11. Abdallah, M., A. P. Freundorfer, and Y. M. M. Antar, "A planar low-cost electrically small antenna for NB-IoT sensors," *2020 IEEE International Symposium on Antennas and Propagation and North American Radio Science Meeting*, 593–594, Montreal, QC, Canada, 2020, doi: 10.1109/IEEECONF35879.2020.9330268.
12. Hossen, M. S. and S. Noman, "On the development of multiband NB-IoT antenna for low-power wide area network terminal," *2022 IEEE 10th Region 10 Humanitarian Technology Conference (R10-HTC)*, 414–418, Hyderabad, India, 2022, doi: 10.1109/R10-HTC54060.2022.9929726.
13. Santamaria, L., F. Ferrero, R. Staraj, and L. Lizzi, "Electronically pattern reconfigurable antenna for IoT applications," *IEEE Open Journal of Antennas and Propagation*, Vol. 2, 546–554, 2021, doi: 10.1109/OJAP.2021.3073104.
14. Tangjitjetsada, M., T. Suangun, W. Chanwattanapong, C. Mahatthanajatuphat, K. Phimthai, and P. Akkaraekthalin, "A multiband tri-branch monopole antenna base on step impedance technique for WLAN, WiMAX, 5G technology, and IoT application," *2023 20th International Conference on Electrical Engineering/Electronics, Computer, Telecommunications and Information Technology (ECTI-CON)*, 1–4, Nakhon Phanom, Thailand, 2023, doi: 10.1109/ECTI-CON58255.2023.10153358.
15. Al-Omari, M., H. Attia, K. K. Qureshi, and S. I. M. Sheikh, "Design of frequency-reconfigurable antenna on dielectric and magnetic metamaterial composite substrate," *IEEE Antennas and Wireless Propagation Letters*, Vol. 22, No. 4, 943–947, April 2023, doi: 10.1109/LAWP.2022.3230827.
16. Lakrit, S., S. Das, B. T. P. Madhav, and K. Vasu Babu, "An octagonal star-shaped flexible UWB antenna with band-notched characteristics for WLAN applications," *Journal of Instrumentation*, 15, P02021, 2020.
17. Sau, P. C., P. K. Sharma, T. J. V. S. Rao, E. K. Kumari, T. V. N. L. Aswini, S. Jindal, and D. Sharma, "A kagome crest fractal optimized quad-band antenna for wireless applications," *Traitement du Signal*, Vol. 40, No. 2, 719–726. 2023.
18. El Yassini, A., M. A. Jallal, S. Ibnyaich, A. Zeroual, and S. Chabaa, "A miniaturized CPW-fed reconfigurable antenna with a single-dual band and an asymmetric ground plane for switchable band wireless applications," *Traitement du Signal*, Vol. 37, No. 4, 633–638, 2020.
19. Li, Y., Z. Zhao, Z. Tang, and Y. Yin, "Differentially fed, dual-band dual-polarized filtering antenna with high selectivity for 5G sub-6 GHz base station applications," *IEEE Transactions on Antennas and Propagation*, Vol. 68, 3231–3236, 2020, doi:10.1109/tap.2019.2957720.
20. Darimireddy, N. K., R. Ramana Reddy, and A. Mallikarjuna Prasad, "Asymmetric triangular semi-elliptic slotted patch antennas for wireless applications," *Radioengineering*, Vol. 27, 85–93, 2018, doi:10.13164/re.2018.0085.
21. Sharma, M., Y. K. Awasthi, and H. Singh, "Design of CPW-fed high rejection triple band-notch UWB antenna on silicon Substrate with diverse wireless applications," *Progress In Electromagnetics Research C*, Vol. 74, 19–30, 2017.
22. Sharawi, M. S., "Current misuses and future prospects for printed multiple-input, multiple-output antenna systems [Wireless Corner]," *IEEE Antennas and Propagation Magazine*, Vol. 59, 162–170, 2017, doi:10.1109/map.2017.2658346.
23. Sneha, P. K. Malik, and A. Alkhayyat, "Correction to: A shared patch mimo antenna for NB-IoT applications," *Low Power Architectures for IoT Applications. Springer Tracts in Electrical and Electronics Engineering*, D. K. Sharma, R. Sharma, G. Jeon, Z. Polkowski, eds., Springer, Singapore, 2023, https://doi.org/10.1007/978-981-99-0639-0_15.
24. Asadpor, L. and M. Rezvani, "Multiband microstrip MIMO antenna with CSRR loaded for GSM and LTE applications," *Microwave and Optical Technology Letters*, Vol. 60, 3076–3080, 2018,

doi:10.1002/mop.31420.

25. Chouhan, S., D. K. Panda, M. Gupta, and S. Singhal, "Meander line MIMO antenna for 5.8 GHz WLAN application," *International Journal of RF and Microwave Computer-Aided Engineering*, Vol. 28, No. 4, e21222, 2018, doi:10.1002/mmce.21222.
26. Mohammad Saadh, A. W., R. Poonkuzhali, and T. Ali, "A miniaturized single-layered branched multiple-input multiple-output antenna for WLAN/WiMAX/INSAT applications," *Microwave and Optical Technology Letters*, Vol. 61, 1058–1064, 2019, doi:10.1002/mop.31652.
27. Wang, M., L. Yang, and Y. Shi, "A dual-port microstrip rectenna for wireless energy harvest at LTE band," *AEU — International Journal of Electronics and Communications*, Vol. 126, 153451, 2020, doi: 10.1016/j.aeue.2020.153451.
28. Sneha, et al., "A metamaterial based monopole antenna for satellite based navigation applications," *International Journal of Intelligent Communication, Computing, and Networks*, Vol. 1, 10–14, 2020, doi:10.51735/ijiccn/001/07.
29. Singh, H., N. Mittal, A. Gupta, Y. Kumar, M. Woźniak, and A. Waheed, "Metamaterial integrated folded dipole antenna with low SAR for 4G, 5G, and NB-IoT applications," *Electronics*, Vol. 10, No. 21, 2612, 2021, doi:10.3390/electronics10212612.
30. PourghorbanSaghati, A., M. Azarmanesh, and R. Zaker, "A novel switchable single- and multifrequency triple-slot antenna for 2.4-GHz bluetooth, 3.5-GHz WiMax, and 5.8-GHz WLAN," *IEEE Antennas and Wireless Propagation Letters*, Vol. 9, 534–537, 2010, doi:10.1109/lawp.2010.2051401.
31. Kulkarni, J., "Multi-band printed monopole antenna conforming bandwidth requirement of GSM/WLAN/WiMAX standards," *Progress In Electromagnetics Research Letters*, Vol. 91, 59–66, 2020.
32. Birwal, A., S. Singh, B. K. Kanaujia, and S. Kumar, "Broadband CPW-fed circularly polarized antenna for IoT-based navigation system," *International Journal of Microwave and Wireless Technologies*, Vol. 11, 835–843, 2019, doi:10.1017/s1759078719000461.
33. Birwal, A., S. Singh, B. K. Kanaujia, and S. Kumar, "Broadband CPW-fed circularly polarized antenna for IoT-based navigation system," *International Journal of Microwave and Wireless Technologies*, Vol. 11, 835–843, 2019, doi:10.1017/s1759078719000461.
34. Raveendra, M., U. Saravanakumar, V. Choppa, N. V. Palivela, and R. Teja, "Design and analysis of a tunable rectangular microstrip slot antenna for narrow band internet of things applications at 1800 MHz," *Antenna Design for Narrowband IoT*, 43–57, January 2022, DOI:10.4018/978-1-7998-9315-8.ch004.
35. Hussain, R., S. I. Alhuwaimel, A. M. Algarni, K. Aljaloud, and N. Hussain, "A compact sub-GHz wide tunable antenna design for IoT applications," *Electronics*, Vol. 11, No. 7, 1074, 2022, doi:10.3390/electronics11071074.
36. Abdulkawi, W. M., A. F. A. Sheta, I. Elshafiey, and M. A. Alkanhal, "Design of low-profile single- and dual-band antennas for IoT applications," *Electronics*, Vol. 10, No. 22, 2766, 2021, doi:10.3390/electronics10222766.
37. Sneha, P., K. Malik, and A. Gehlot, "A key-shaped ultra-wideband antenna for IoT applications," *2023 International Conference on Artificial Intelligence and Smart Communication (AISC)*, 504–508, Greater Noida, India, 2023, doi: 10.1109/AISC56616.2023.10085314.
38. Althuwayb, A. A., M. Alibakhshikenari, B. S. Virdee, P. Shukla, and E. Limiti, "Realizing UWB antenna array with dual and wide rejection bands using metamaterial and electromagnetic bandgaps techniques," *Micromachines*, Vol. 12, No. 3, 269, Basel, 2021, doi:10.3390/mi12030269.
39. Balanis, C. A., *Antenna Theory: Analysis and Design*, 3rd Edition, John Wiley, Hoboken, NJ, 2005.
40. Zhuo, L., H. Han, X. Shen, and H. Zhao, "A U-shaped wide-slot dual-band broadband NB-IoT antenna with a rectangular tuning stub," *2020 IEEE 4th Information Technology, Networking, Electronic and Automation Control Conference (ITNEC)*, 123–128, 2020, doi: 10.1109/ITNEC48623.2020.9084751.